International Journal of Minerals, Metallurgy and Materials
Volume 28, Number 12, December 2021, Page 1898
https://doi.org/10.1007/s12613-020-2158-1

New insights into the flotation responses of brucite and serpentine for different conditioning times: Surface dissolution behavior

Ya-feng Fu[1,2], *Wan-zhong Yin*[2], *Xian-shu Dong*[1], *Chuan-yao Sun*[3], *Bin Yang*[2], *Jin Yao*[2], *Hong-liang Li*[1,4], *Chuang Li*[2], *and Hyunjung Kim*[5]

1) College of Mining Engineering, Taiyuan University of Technology, Taiyuan 030024, China
2) School of Resources & Civil Engineering, Northeastern University, Shenyang 110819, China
3) State Key Laboratory of Mineral Processing, Beijing 102628, China
4) Department of Chemical and Materials Engineering, University of Alberta, Edmonton, Alberta T6G 2V4, Canada
5) Department of Mineral Resources and Energy Engineering, Jeonbuk National University, Baekje-daero, Deokjin-gu, Jeonju-si, Jeollabuk-do, 561-756, Republic of Korea
(Received: 7 May 2020; revised: 6 August 2020; accepted: 7 August 2020)

Abstract: The inadvertent dissolution of gangue minerals is frequently detrimental to the flotation of valuable minerals. We investigated the effect of conditioning time on the separation of brucite and serpentine by flotation. By analyzing the Mg^{2+} concentration, relative element content, and pulp viscosity, we studied the effect of mineral dissolution on brucite flotation. The results of artificially mixed mineral flotation tests (with −10 μm serpentine) showed that by extending the conditioning time from 60 to 360 s, a large amount of Mg^{2+} on the mineral surface gradually dissolved into the pulp, resulting in a decreased brucite recovery (from 83.83% to 76.79%) and an increased recovery of serpentine from 52.12% to 64.03%. To analyze the agglomeration behavior of brucite and serpentine, we used scanning electron microscopy, which clearly showed the different adhesion behaviors of different conditioning times. Lastly, the total interaction energy, as determined based on the extended DLVO (Derjaguin–Landau–Verwey–Overbeek) theory, also supports the conclusion that the gravitational force between brucite and serpentine increases significantly with increased conditioning time.

Keywords: surface dissolution; flotation; brucite; serpentine; entrainment; E-DLVO theory

1. Introduction

Magnesium is a lightweight metallic material with a high specific strength and elastic modulus, excellent damping, and good machinability [1]. Brucite is one of the main types of mined magnesium resources. Because of its chemical properties, which are superior to that of magnesite, it is typically used as an electrical material and advanced refractory. For many years, with the transitioning exploitation of mineral resources, high-purity brucite resources have been increasingly depleted, and a large amount of low-grade brucite in association with serpentine is now mined. Serpentine, due to its layered structure and low hardness, is prone to over-grinding in grinding operations. Thus, a considerable amount of serpentine mud is produced [2–3], which seriously degrades the pulp environment during the flotation of brucite. As such, the development of a method to reduce the influence of fine-grained serpentine has become a major challenge for realizing the efficient development and utilization of low-grade brucite resources.

It is well known that the serpentine in gangue minerals often interferes with the separation of valuable minerals by flotation. Liu *et al.* [4] believed that lemon yellow could be used to selectively adsorb onto the serpentine surface by electrostatic interaction, and thus efficiently limit its detrimental effect on pyrite flotation. Low-molecular-weight anionic sodium polyacrylate can selectively adsorb onto the serpentine surface, thereby changing its surface potential as well as the interactions between pyrite and serpentine [5]. In view of the difficulty of suppressing serpentine during the flotation of pentlandite, Edwards *et al.* [6] reported that chemical reagents that modified serpentine's surface charge could be effective in reducing the adverse influence of serpentine during pentlandite flotation. Feng *et al.* [7] proposed that an appropriate amount of quartz could be added to the pulp to adsorb the fine serpentine particles onto the quartz

Corresponding authors: Hong-liang Li E-mail: honglia1@ualberta.ca; Chuang Li E-mail: 13514209873@163.com

surface, thereby limiting their detrimental effect. Bobicki *et al.* [8] believed that microwave pre-treatment could reduce the slurry viscosity and yield stress of the flotation pulp. Because graphene oxide contains multiple oxygen-containing functional groups, it can be selectively adsorbed onto the serpentine surface, thereby inhibiting its floatability and reducing the content of serpentine in the flotation concentrate [9]. In addition, as serpentine is extremely prone to over-grinding, non-selective entrainment is the main reason for fine serpentine entering the flotation concentrate [10–11].

In general, the separation of valuable minerals from a mixture containing serpentine is difficult mainly because of the dissolution, hydrolysis, and adsorption behavior of serpentine in solution, which results in the serious adhesion of serpentine onto valuable minerals, which is usually called "slime coating." Tartaj *et al.* [12] investigated the isoelectric point and Mg/Si atomic ratio of the serpentine surface in solution, and determined that the dissolution of ions has a significant effect on the water/serpentine electrical interface. Irannajad *et al.* [13] believed that surface dissolution had a significant effect on oxide and silicate minerals, and that the dissolution time should be as short as possible to obtain the desired flotation concentrate. Zhu *et al.* [14] noted that cations or anions can be dissolved and transferred from the mineral surface into the pulp, resulting in a change in the surface electrochemistry of minerals. Tang and Chen [15] proposed that after conditioning with oxalic acid, the surface of serpentine is negatively charged such that its slime coatings on the surface of pyrite are eliminated. Alvarez-Silva [16] believed that the dissolution of Mg^{2+} on the surface of serpentine can activate the floatability of pentlandite. Cao *et al.* [17] reported that neither Cu^{2+} and Ni^{2+} can activate the floatability of serpentine under acidic conditions, whereas, in alkaline solutions, $Cu(OH)_2$ and $Ni(OH)_2$ are adsorbed onto the serpentine surface, thus facilitating the recovery of serpentine. In addition, the presence of serpentine significantly increases the viscosity of the pulp, and the dissolution of serpentine can be accelerated under acidic conditions, thus alleviating the impact of serpentine on pulp rheology [18].

The authors of other studies [19–20] have indicated that brucite silicification is a fundamentally rate-limiting elementary reaction for the production of both serpentine and talc from forsterite in nature, which leads to surface properties extremely similar to those of brucite and serpentine. Ding *et al.* [21] found that Mg^{2+} is the active site for the reaction of brucite with the collector, thereby enabling the effective separation of brucite and serpentine. Fluoride ions in fluorosilicate can corrode Mg^{2+} from the surfaces of brucite and serpentine, which prevents the collectors from adsorbing onto the mineral surface [22]. The hydrolysate, $SiO(OH)_3^-$, of sodium silicate selectively adsorbs onto serpentine, thus inhibiting its floatability during brucite flotation [23]. However, although both serpentine and brucite in solution exhibit serious dissolution behavior, few papers refer to the effect of serpentine dissolution on brucite flotation.

Mineral dissolution behavior plays an important role in aqueous solutions, especially in salt minerals, and dissolved ions always undergo further reactions such as adsorption, complexation, hydrolysis, or bulk precipitation. Due to the continuous dissolution and adsorption of ions onto the surface of brucite and serpentine in pulp, the surface properties of these two minerals tend to be the same after long stirring times, which further increases the difficulty of separating brucite and serpentine during flotation. The objective of this paper is to explore the effective separation of brucite from serpentine by flotation, with particular attention to the change in the agglomeration states of brucite and serpentine after different conditioning times.

2. Experimental

2.1. Materials and reagents

Pure brucite and serpentine samples were obtained from Dandong City (Liaoning province, China). The high-grade raw ores were carefully crushed, and high-crystallinity ore was manually selected and then ground by a ceramic ball mill to obtain samples with different size fractions. Four size fractions (−74+45 μm, −45+25 μm, −25+10 μm, and −10 μm) were generated by elutriation and sieving methods. X-ray diffraction (Fig. 1) and multi-element chemical analysis (Table 1) confirmed that the purities of the brucite and serpentine samples were greater than 95%.

We purchased sodium oleate (NaOl), hydrochloric acid (HCl), sodium hydroxide (NaOH), and magnesium chloride ($MgCl_2$) of analytical grade from Kermil Chemical Reagents Development Center, Tianjin, China. Distilled water was employed in all the experiments.

2.2. Artificially mixed mineral flotation tests

We conducted artificially mixed mineral flotation tests in a flotation apparatus (Fig. 2). This device can effectively increase the collision probability of valuable minerals and bubbles and reduce the non-selective entrainment of gangue minerals by lengthening the floating paths of the bubbles [24]. This enables more accurate analysis of the flotation behavior of the minerals.

In the typical artificially mixed mineral flotation test, we prepared the mineral pulp by adding 2 g of a mineral sample (1.5 g brucite and 0.5 g serpentine) into a 50-mL breaker with 50 mL of distilled water and then stirring for 2 min, followed by 2 min of conditioning after the addition of sodium oleate. Subsequently, the suspension was transferred to the tube and floated for 3 min with a fixed nitrogen flow rate of 0.4 L/min. The froth products (m_1) and tailings were sequentially dried and weighed, and the SiO_2 content (β, X-ray fluorescence spectrometry) in the foam products were analyzed. The re-

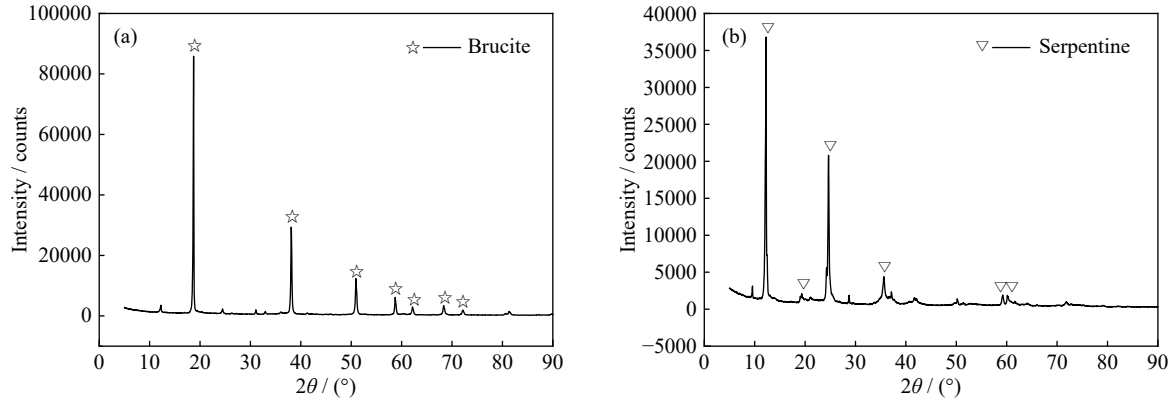

Fig. 1. XRD patterns of brucite (a) and serpentine (b).

Table 1. Multi-element chemical analysis of pure minerals wt%

Minerals	MgO	CaO	SiO_2	FeO	Al_2O_3	LOI
Brucite	66.23	0.98	0.82	0.33	0.03	30.97
Serpentine	41.75	0.87	44.71	0.27	0.12	14.38

Note: LOI—Loss on ignition.

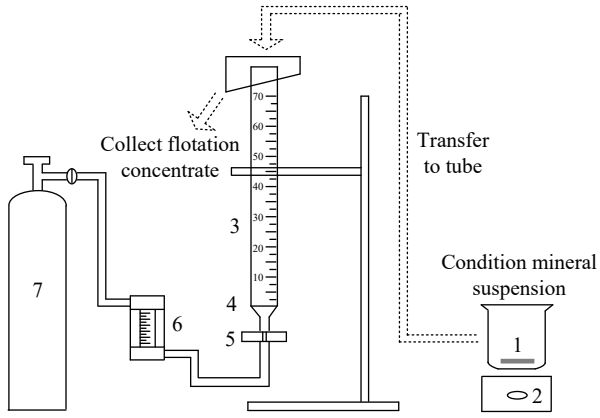

Fig. 2. Schematic diagram of the flotation apparatus (pore diameter of microporous core: 40–50 μm).

coveries of brucite (γ_1) and serpentine (γ_2) in the foam products can therefore be derived as follows:

$$\gamma_1 = (m_1 - \frac{m_1\beta}{0.4471})/1.5 \times 100\% \quad (1)$$

$$\gamma_2 = \frac{m_1\beta/0.4471}{0.5} \times 100\% \quad (2)$$

2.3. Mineral dissolution analyses

The mineral dissolution analyses performed in this study were based on the changes in the pH, Mg^{2+} concentration in the supernatant, relative element content on the mineral surface, and pulp viscosity.

2.3.1. Pulp pH measurements

We mixed 2 g of mineral (brucite or serpentine) with 50 mL of distilled water in a 50-mL beaker. The pulp pH was measured at a stirring speed of 600 r/min until a stable reading was obtained.

2.3.2. Measurements of Mg^{2+} concentration and relative element contents

Prior to the test, we added pure serpentine (5 g) to a beaker with 50 mL of distilled water, which was conditioned for a specified time. Afterwards, the suspension was centrifuged and the supernatant was analyzed to obtain the Mg^{2+} concentration using an Optima 4300DV inductive coupled plasma emission spectrometer (ICP, PE Co.). The precipitate (−10 μm serpentine) was air-dried and investigated using a VG ESCALAB MK II X-ray photoelectron spectroscopy (XPS) analyzer to determine the relative contents of the elements on the serpentine surface [25].

2.3.3. Pulp viscosity measurements

We measured the pulp viscosity using a BROOKFIELD DV2T rotary viscometer. Then, we suspended 20 g of the mineral sample in 500 mL of distilled water, and obtained the pulp viscosity after conditioning with a magnetic stirrer (600 r/min) for a specified duration. For the measurements, the viscometer rotation speed was adjusted to 200 r/mim. We measured the pulp viscosity under each condition at least three times and calculated the average value.

2.4. Zeta potential measurements

Zeta potential measurements were performed using a Malvern Instruments Nano-ZS90 zeta potential analyzer. Prior to the test, 20 mg of the mineral sample (−5 μm) was conditioned in 50 mL of KCl solution (1×10^{-3} mol/L). The pulp pH was regulated with either HCl or NaOH solution. The zeta potential was measured after conditioning with a magnetic stirrer for a specified duration. At least five measurements were performed for each condition, from which we

calculated and reported the mean and standard deviation of the zeta potential.

2.5. Contact angle measurements

The contact angle is commonly used to characterize the wettability of a material, with the advancing contact angle deemed to be the approximately ideal Young's contact angle. To minimize the influence of the surface roughness and heterogeneity on the contact angle of the sample during measurement, after grinding, the samples were polished with a 0.05-μm alumina powder solution. Then, we measured the advancing contact angles of serpentine for different conditioning times and analyzed its dissolution [26].

Contact angle measurements were performed on a JC2000A contact angle analyzer using the sessile drop method. After centrifugation of the pulp with sodium oleate for different conditioning times, we vacuum dried the precipitate at 40°C for 24 h. Afterwards, the minerals were embedded in resin and ground with a diamond grinding disc to obtain a flat surface, which was then further polished with a 0.05-μm alumina powder solution [27–28]. During the measurement, we dispensed a stable and suitable water droplet of approximately 4.5 μL from a micro-syringe and measured the contact angle of the water droplets on the flat surface by capturing an image of the droplet profile. We performed at least five measurements on each sample surface and recorded the average value.

2.6. Scanning electron microscopy observation

To investigate the agglomeration behavior of particles more intuitively, we examined the vacuum-dried samples by scanning electron microscopy (SEM, ULTRA PLUS, ZEISS). The mineral particles (1.5 g brucite (−74+45 μm) and 0.5 g serpentine (−10 μm)) were mixed with 50 mL of distilled water in a 50-mL beaker and the pulp was stirred for a specified duration after adding sodium oleate. Then, using a syringe, 2 mL of homogeneous solution was siphoned from the middle of the beaker, transferred to a glass plate, and then vacuum dried for observation. This method enables a more intuitive and accurate understanding of the agglomeration behavior of particles in the pulp.

3. Results and discussion

3.1. Effect of conditioning time on the recovery of brucite and serpentine

In the artificially mixed mineral flotation tests, we investigated the effect of conditioning time on the flotation performance of brucite and serpentine, the results of which are shown in Fig. 3. The experimental results indicate that the conditioning time has a significant effect on the recovery of brucite and serpentine. Interestingly, with an increase in the conditioning time, the brucite recovery tended to decrease whereas the serpentine recovery gradually increased. For example, with the −10 μm serpentine mixture, the recovery of brucite decreased from 83.83% (conditioning for 60 s) to 76.79% (conditioning for 360 s), and that of serpentine increased from 52.12% (conditioning for 60 s) to 64.03% (conditioning for 360 s), an increase of 11.91%. In addition, the experimental results demonstrate that fine-grained serpentine has a stronger inhibitory effect on brucite than coarse-grained serpentine.

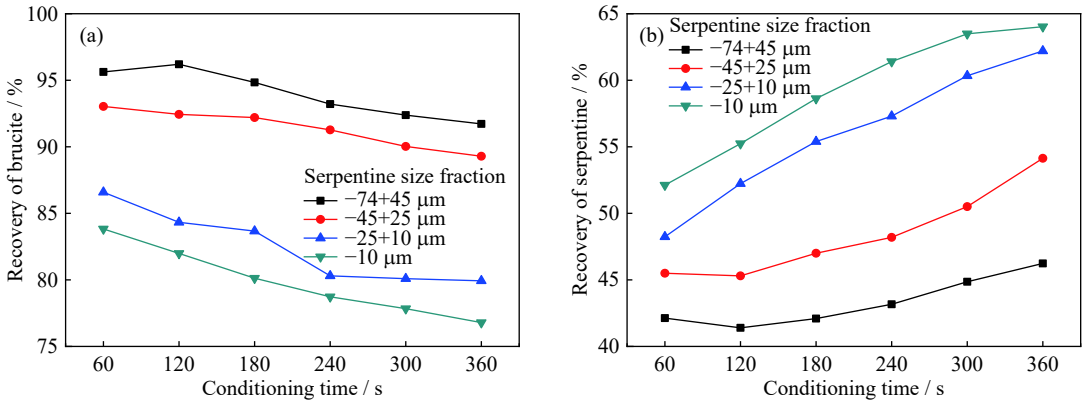

Fig. 3. Effect of conditioning time on the recovery of (a) brucite and (b) serpentine (the size fraction of brucite: −74+45 μm; sodium oleate dosage: 200 mg/L; pulp pH value: 10; stirring speed: 600 r/min).

3.2. Mineral dissolution analyses

In view of the fact that conditioning time seriously affects the artificially mixed mineral flotation performance, we investigated the mechanism of this process by mineral dissolution analyses of the pulp pH, Mg^{2+} concentration in the supernatant, relative content of elements on the mineral surface, and pulp viscosity.

3.2.1. Pulp pH

As shown in Fig. 4(a), the pH value of the −74+45 μm brucite pulp generally remained at 10.1 after conditioning for 20 s, whereas that of the −10 μm brucite was stable after conditioning for just 9 s. These results indicate that as the particle size of brucite decreased, the dissolution rate increased. Ser-

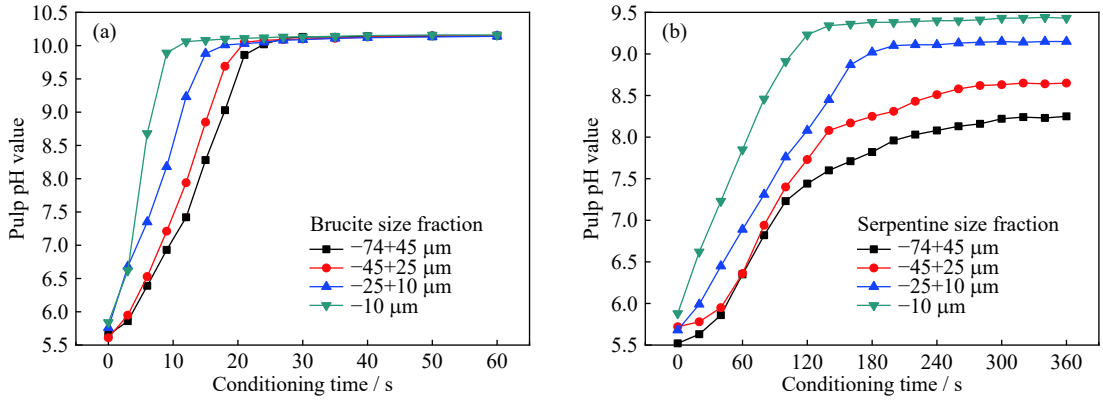

Fig. 4. Effect of conditioning time on pH values of the brucite (a) and serpentine (b) pulps.

pentine has a similar dissolution rate (Fig. 4(b)). After conditioning for 240 s, the pH value of the −74+45 μm serpentine pulp stabilized at about 8.0, whereas that of the −10 μm serpentine remained at about 9.3 after conditioning for 150 s. These results reveal that the dissolution rate of the fine-grained serpentine was significantly higher than that of the coarse-grained serpentine, and the final pulp pH of the fine-grained serpentine was dramatically higher than that of the coarse-grained serpentine.

In addition, and even more importantly, the dissolution rate of brucite is significantly higher than that of serpentine. After conditioning for just 20 s, the pH of the brucite pulp remained stable, whereas the serpentine pulp required conditioning for approximately 150 s for the pH to stabilize.

3.2.2. Mg^{2+} concentration in supernatant

Conditioning time is known to have a significant influence on the dissolution of salt minerals in solution [7,29–31]. Fig. 5 shows the effect of conditioning time on the Mg^{2+} concentration in the serpentine supernatant. We can see that the Mg^{2+} concentration in the serpentine pulp gradually increased with conditioning time for both the coarse-grained and fine-grained serpentine. In addition, the Mg^{2+} concentration in the fine-grained serpentine solution supernatant was obviously higher than that of the coarse one. The Mg^{2+} concentration in the −10 μm serpentine pulp reached 4.32 mg/L, whereas that in the −74+45 μm serpentine pulp only reached 3.45 mg/L. Previous studies [32–33] have reported that the oleate anion in solution is prone to react with Mg^{2+}, resulting in a decrease in the concentration of the collector available for adsorption onto the minerals. Therefore, the inhibitory mechanism may be that the dissolved Mg^{2+} in the pulp consumes a large amount of oleate anions, which leads to a dramatic reduction in the recovery of brucite.

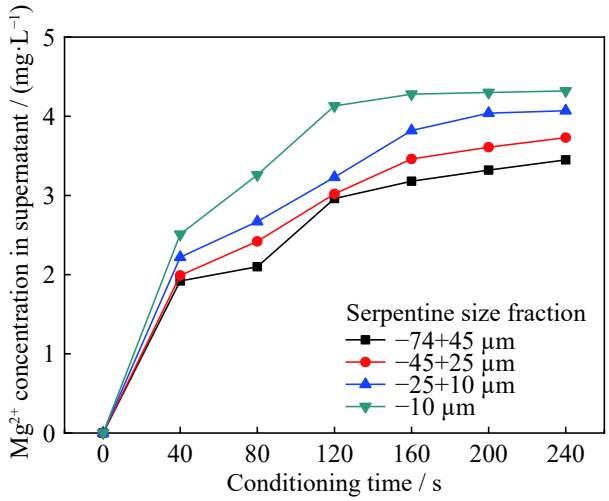

Fig. 5. Effect of conditioning time on Mg^{2+} concentration in serpentine supernatant.

3.2.3. Relative element contents

XPS, an advanced analytical technology, is commonly used to investigate the valence states of elements on particle surfaces and in the semi-quantitative analysis of surface elements. This technique is widely applied in the materials, leaching, and chemical industries [28,34].

In this work, we used XPS to investigate the influence of conditioning time on the relative element contents on the serpentine surface, the results of which are summarized in Table 2. It is reasonable to conclude that the relative content of Mg on the serpentine surface gradually decreased with increasing conditioning time (C is derived from CO_2 in the air). The content of Mg on the serpentine surface (without stirring) was 21.62at%. After conditioning for 180 s, the relative content of Mg had reduced to 18.67at%, a decrease of 2.95at%. The results in Table 2 also indicate that the Mg on the serpentine surface was being continuously dissolved and integrated into the pulp.

Table 2. Relative contents of elements on the surface of −10 μm serpentine as determined by XPS at%

Conditioning time / s	C	O	Mg	Si
0	13.18	52.84	21.62	12.36
60	15.02	52.78	20.05	12.15
120	15.86	52.86	18.96	12.32
180	16.31	52.81	18.67	12.21

3.2.4. Pulp viscosity

Generally, suspensions of serpentine minerals have high viscosity and yield stress, and the dissolution of serpentine has a significant effect on the pulp viscosity [8,35]. Thus, we investigated the effect of conditioning time on the serpentine pulp viscosity, the results of which are shown in Fig. 6. We can see that the pulp viscosity increased significantly with increases in the conditioning time, especially for the −10 μm serpentine size fraction, whose pulp viscosity increased from 7.35 mPa·s (conditioning for 30 s) to 13.82 mPa·s (conditioning for 180 s). Therefore, it is reasonable to conclude that the viscosity of serpentine pulp increases after conditioning for a specified time, and the foam stability is enhanced [36], which results in an increase in serpentine entrainment during flotation [37–38]. This finding is consistent with those of previous reports [35].

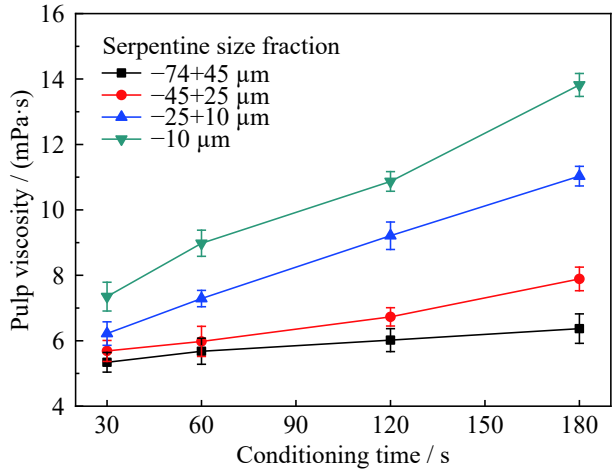

Fig. 6. Effect of conditioning time on pulp viscosity in serpentine supernatant. Error bars denote 2σ error.

3.3. Observation of particle agglomeration behavior

The above results indicate that the surface dissolution of serpentine significantly affects the physicochemical properties of the mineral surface and the recovery of brucite, the mechanism of which was considered based on SEM observations and extended Derjaguin–Landau–Verwey–Overbeek (E-DLVO) theory calculations. Fig. 7 shows SEM images that illustrate the particle agglomeration behaviors of brucite and serpentine after different conditioning times. We found that virtually no fine-grained serpentine adhered to the brucite surface in the initial stage (Fig. 7(a)). However, with an increase in the conditioning time, the content of fine-grained serpentine on the surface of the brucite had obviously increased, and a "slime coating" gradually appeared on the brucite surface (Fig. 7(d)). The reason for this may be that a large amount of Mg^{2+} on the surface of the serpentine had dis-

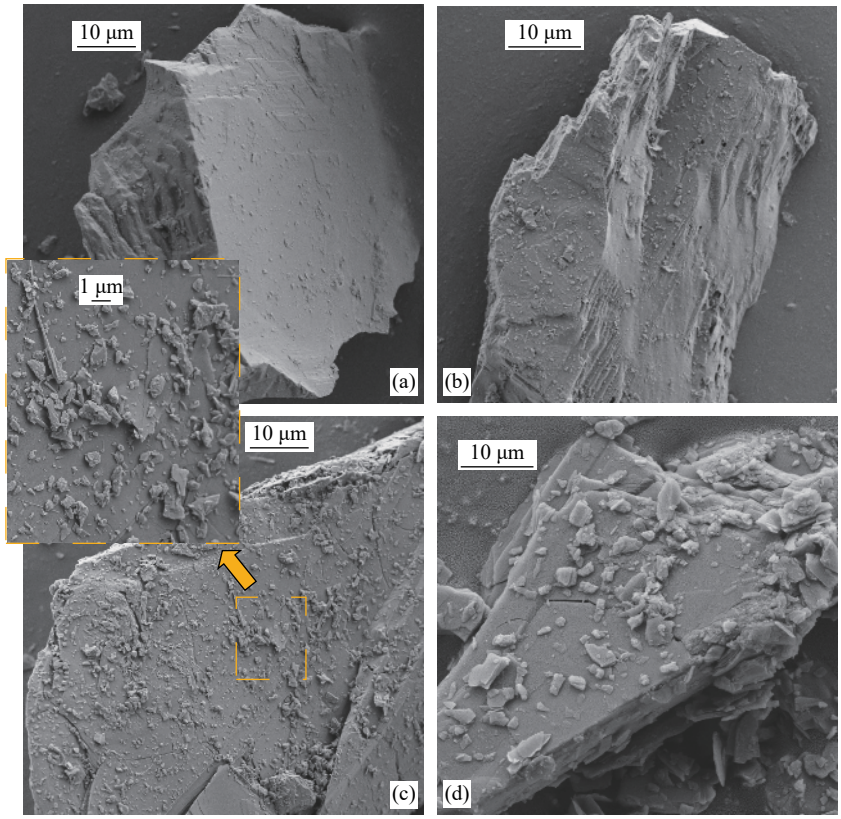

Fig. 7. SEM images of brucite and serpentine conditioned for (a) 0 s, (b) 60 s, (c) 120 s, and (d) 180 s (sodium oleate dosage: 200 mg/L; stirring speed: 600 r/min; brucite size: −74+45 μm; serpentine size: −10 μm).

solved after a long stirring time, which changed the surface potential of the serpentine [39] and affected the interaction force between serpentine and brucite, resulting in entirely different adhesion behaviors by brucite and serpentine in the solution.

3.4. E-DLVO theoretical calculations

Based on the flotation results (Fig. 3) and the observed particle agglomeration behavior (Fig. 7), it is reasonable to consider that conditioning time has a significant effect on the adhesion behaviors of brucite and serpentine in pulp. The classical DLVO theory can be used to understand the stability of charged colloidal particles by analyzing the electrostatic and van der Waals forces between colloidal particles [40]. However, the stability cannot be well explained when the particle surfaces are extremely hydrophilic (or hydrophobic). However, the extended DLVO (E-DLVO) theory not only takes into account the electrostatic and van der Waals interactions, but also the polar interfacial and hydrophobic interactions, which can be used to elucidate the agglomeration behavior of particles under certain conditions [41]. Therefore, in this study, we applied the E-DLVO theory to calculate the interaction forces between brucite and serpentine after different conditioning times. The total interaction energy (V_T^{ED}) is calculated using Eq. (3):

$$V_T^{ED} = V_W + V_E + V_H \tag{3}$$

where V_W is the van der Waals interaction, V_E is the electrical interaction, and V_H is the hydrophobic (or hydration) interaction.

(1) The van der Waals interaction, V_W, is calculated as follows:

$$V_W = -\frac{A_{132}}{6H}\frac{R_1R_2}{R_1+R_2} \tag{4}$$

where R_1 and R_2 are the radius of the brucite and serpentine particles, respectively; H is the distance between two spherical particles; and A_{132} is the effective Hamaker constant, which is defined as follows:

$$A_{132} = \left(\sqrt{A_{11}} - \sqrt{A_{33}}\right)\left(\sqrt{A_{22}} - \sqrt{A_{33}}\right) \tag{5}$$

where A_{11}, A_{22}, and A_{33} are the Hamaker constants of brucite (0.38×10^{-20} J), serpentine (22.8×10^{-20} J), and water (4.0×10^{-20} J) in a vacuum, respectively [42–44].

(2) The electrostatic interaction, V_E, is calculated as follows:

$$V_E = \frac{\pi\varepsilon_0\varepsilon_r R_1R_2}{R_1+R_2}(\varphi_1^2+\varphi_2^2)\left[\frac{2\varphi_1\varphi_2}{\varphi_1^2+\varphi_2^2}p+q\right] \tag{6}$$

where

$$p = \ln\left[\frac{1+\exp(-\kappa H)}{1-\exp(-\kappa H)}\right] \tag{7}$$

$$q = \ln[1-\exp(-2\kappa H)] \tag{8}$$

where ε_0 and ε_r are the permittivities in the vacuum (8.854×10^{-12} $C^{-2}\cdot J^{-1}\cdot m^{-1}$) and solution (for water ε_r = 78.5 $C^{-2}\cdot J^{-1}\cdot m^{-1}$), respectively; κ^{-1} is the Debye length, which equals 0.104 nm^{-1}; φ_1 and φ_2 are the respective surface potentials of brucite and serpentine, which can be calculated by following formula:

$$\varphi = \zeta(1+\chi/R)\exp(\kappa\chi) \tag{9}$$

where ζ is the zeta potential (Fig. 8), and χ is 5×10^{-10} m [44].

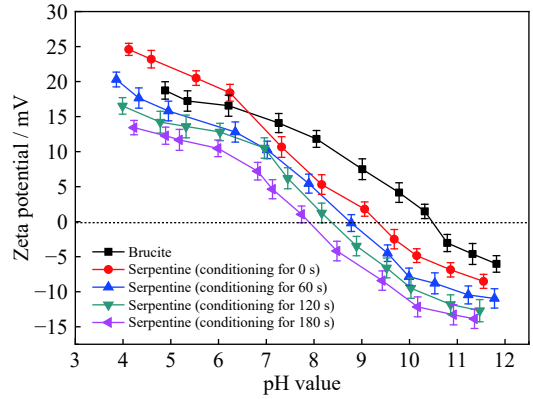

Fig. 8. Zeta potentials of brucite and serpentine as a function of pH value (KCl dosage: 1×10^{-3} mol/L). Error bars denote 2σ error.

(3) The hydrophobic (or hydration) interaction, V_H, is calculated as follows:

$$V_H = 2\pi\frac{R_1R_2}{R_1+R_2}h_0V_H^0\exp\left(\frac{H_0-H}{h_0}\right) \tag{10}$$

where H_0 is the equilibrium contact distance (H_0 = 0.2 nm); h_0 is the attenuation length, which is generally approximated to be 1 nm; and V_H^0 is the interaction energy of the polar interface, which is defined as follows:

$$V_H^0 = 2\left[\sqrt{\gamma_L^+}\left(2\sqrt{\gamma_S^-} - \sqrt{\gamma_L^-}\right) + \sqrt{\gamma_L^-}\left(2\sqrt{\gamma_S^+} - \sqrt{\gamma_L^+}\right) - 2\sqrt{\gamma_S^+\gamma_S^-}\right] \tag{11}$$

where γ_S^+ and γ_L^+ are the electron donor components of the solid and liquid, respectively, and γ_S^- and γ_L^- are the respective electron acceptor components of the solid and liquid.

Based on the work of Ansarinasab and Jamialahmadi [45], we know that the contact angle is a function of the interfacial free energy of the gas, liquid, and solid phases. It is related both to the surface properties of the minerals as well as the polar and apolar components of the liquid and gas phases [46–47], as shown by the following equation:

$$(1+\cos\theta)\gamma_L = 2\left(\sqrt{\gamma_S^d\gamma_L^d} + \sqrt{\gamma_S^+\gamma_L^-} + \sqrt{\gamma_S^-\gamma_L^+}\right) \tag{12}$$

where θ is the contact angle and γ_S^d and γ_L^d are the apolar components of the surface tensions of the solid and liquid, respectively.

Because most oxidized and silicate minerals have unipolar surfaces, that is, $\gamma_S^+ \approx 0$, Eqs. (11) and (12) can be ab-

breviated as follows:

$$V_H^0 = 4\left(\sqrt{\gamma_L^+\gamma_S^-} - \sqrt{\gamma_L^+\gamma_L^-}\right) \quad (13)$$

$$(1+\cos\theta)\gamma_L = 2\left(\sqrt{\gamma_S^d\gamma_L^d} + \sqrt{\gamma_S^-\gamma_L^+}\right) \quad (14)$$

Variable γ_S^d is related to the Hamaker constant A, by [44]:

$$A = 24\pi\gamma_S^d H_0^2 \quad (15)$$

Table 3 presents the surface tension parameters of two polar liquids (water and glycerol), and Fig. 8 shows the zeta potentials of brucite and serpentine. We determined the contact angles of brucite and serpentine, as shown in Table 4, from which it is reasonable to conclude that conditioning time has a significant influence on the hydrophobicity of serpentine.

Table 3. Surface tension parameters of water and glycerin [42–43] (mJ·m^{-2})

Liquid	γ_L	γ_L^+	γ_L^d	γ_L^-
Water	72.8	25.5	21.8	25.5
Glycerol	64	3.92	34	57.4

Table 4. Contact angles of brucite and serpentine (sodium oleate dosage: 200 mg/L) (°)

Measuring medium	Brucite	Serpentine			
		0 s	60 s	120 s	180 s
Water	122.2	95.2	99.7	102.3	103.6
Glycerol	113.5	101.5	104.6	106.7	109.4

Using Eqs. (3)–(15), we calculated the total interaction energy (V_T^{ED}) between brucite and serpentine, the results of which are presented in Fig. 9. As shown in the figure, the total interaction energy between brucite and serpentine in the pulp is negative, i.e., the interaction force between these two mineral particles is gravitational. Furthermore, the gravitational force between brucite and serpentine increased significantly with increased conditioning time, which indicates that serpentine is easily adsorbed onto the surface of brucite after a long conditioning time of the pulp. This results in a decrease in the recovery of brucite and an increase in the recovery of serpentine [48], which is consistent with the results of our artificially mixed mineral flotation tests (Fig. 3) and SEM observations (Fig. 7).

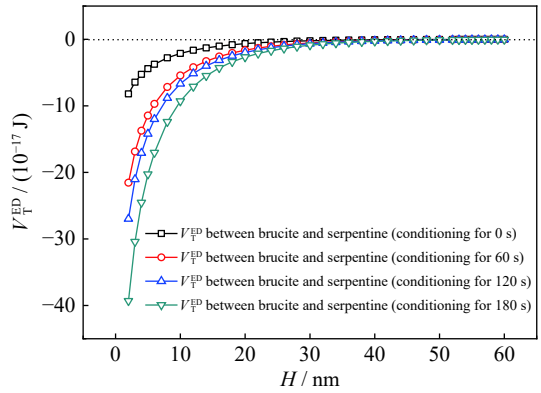

Fig. 9. Total interaction energy between brucite and serpentine (the diameters of brucite and serpentine particles are assumed to be 60 and 5 μm, respectively; pH value is assumed to be 10).

3.5. Analysis of stirring mechanism

The results of the artificially mixed mineral flotation tests indicate that the conditioning time has a significant effect on the recovery of brucite and serpentine. The mineral dissolution tests show that the Mg^{2+} on the serpentine surface slowly dissolves with increased conditioning time, resulting in a change in the surface potential of serpentine and an increase in the gravitational force between brucite and serpentine. Therefore, more serpentine is adsorbed onto the brucite sur-

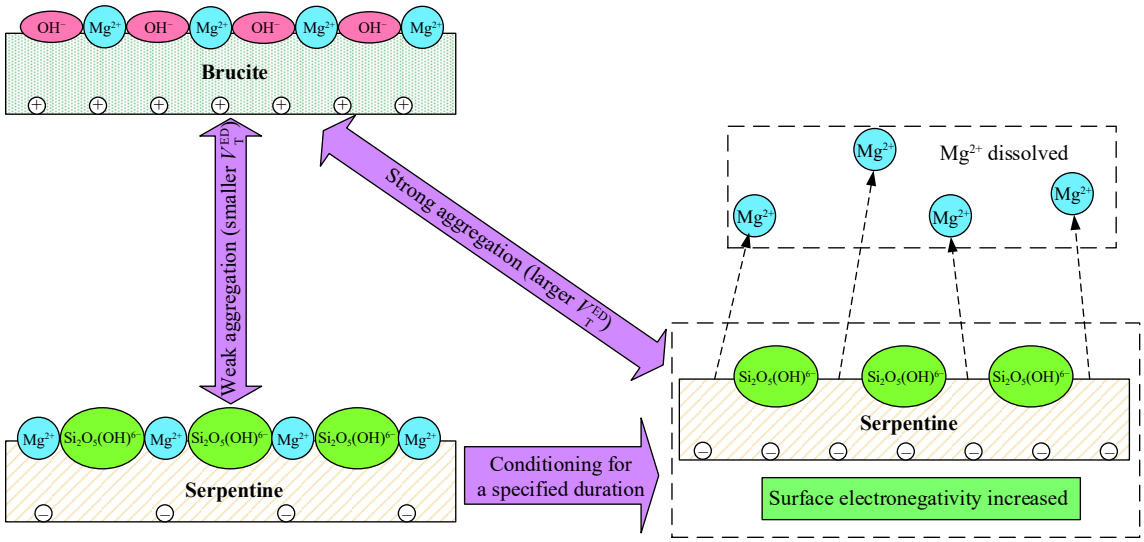

Fig. 10. Schematic diagram of aggregation of brucite and serpentine after conditioning (pulp pH value: 10).

face, which reduces the recovery of brucite and increases that of serpentine. Based on the mineral dissolution analyses of the pulp pH, Mg^{2+} concentration, relative content of elements on the serpentine surface, and pulp viscosity, Fig. 10 shows a schematic of the aggregation of brucite and serpentine before and after conditioning.

4. Conclusions

In this work, batch flotation tests of artificially mixed minerals were investigated using a modified Hallimond tube and the results revealed that long-term conditioning of the pulp will significantly reduce the recovery of brucite. The dissolution behaviors of brucite and serpentine in solution were mainly investigated by ICP, XPS, and a viscometer. We preformed E-DLVO theoretical calculations combined with SEM observations to investigate the mechanism of the conditioning time in the separation of brucite and serpentine by flotation. Several meaningful conclusions were drawn, which can be summarized as follows.

(1) The artificially mixed mineral flotation results indicated that with increases in the conditioning time, the recovery of brucite decreased, whereas that of serpentine increased significantly. For the artificially mixed mineral suspension with −10 μm serpentine, the recovery of brucite decreased from 83.83% (conditioning for 60 s) to 76.79% (conditioning for 360 s), whereas the recovery of serpentine increased from 52.12% (conditioning for 60 s) to 64.03% (conditioning for 360 s). Furthermore, the fine-grained serpentine was found to have a stronger inhibitory effect on brucite flotation than the coarse one.

(2) The pulp pH, Mg^{2+} concentration, and relative content of elements on the serpentine surface revealed that, after a long period of stirring, the dissolved Mg^{2+} in the pulp consumed a large amount of oleate anions, resulting in a dramatic reduction in the recovery of brucite. In addition, the pulp viscosity increased from 7.35 to 13.82 mPa·s after conditioning for 180 s, which resulted in an increase in the serpentine entrainment during froth flotation.

(3) The E-DLVO theoretical calculations indicated that the interaction force between brucite and serpentine is gravitational. Moreover, this gravitational force increased dramatically as the conditioning time increased, which led to a serious "slime coating" on the brucite surface. These results are consistent with those of the flotation tests and SEM observations.

In conclusion, we have provided evidence that a long stirring time seriously reduces the recovery of brucite by flotation by consuming a large amount of oleate anions and increasing the gravitational force between brucite and serpentine. From a broader perspective, our observations may have implications for the application of flash flotation technology (i.e., a shortened flotation time, which would eliminate the influence of salt mineral dissolution on flotation to the degree possible) in the flotation of brucite and serpentine.

Acknowledgements

The authors gratefully acknowledge the financial support from the Project funded by the China Postdoctoral Science Foundation (No. 2020M670709), the National Natural Science Foundation of China (No. 51974064), the Fundamental Research Funds for the Central Universities, China (No. N2101025), and the Open Foundation of State Key Laboratory of Mineral Processing (No. BGRIMM-KJSKL-2017-02).

References

[1] C. Blawert, W. Dietzel, E. Ghali, and G. Song, Anodizing treatments for magnesium alloys and their effect on corrosion resistance in various environments, *Adv. Eng. Mater.*, 8(2006), No. 6, p. 511.

[2] G.I. Pushkaryova, Effect of temperature treatment of brucite on its sorption properties, *J. Min. Sci.*, 36(2000), No. 6, p. 599.

[3] A.M. Kusuma, Q.X. Liu, and H.B. Zeng, Understanding interaction mechanisms between pentlandite and gangue minerals by zeta potential and surface force measurements, *Miner. Eng.*, 69(2014), p. 15.

[4] D.Z. Liu, G.F. Zhang, G.H. Huang, Y.W. Gao, and M.T. Wang, The flotation separation of pyrite from serpentine using lemon yellow as selective depressant, *Colloids Surf. A*, 581(2019), art. No. 123823.

[5] K.L. Zhao, W. Yan, X.H. Wang, G.H. Gu, J. Deng, X. Zhou, and B. Hui, Dispersive effect of low molecular weight sodium polyacrylate on pyrite–serpentine flotation system, *Physicochem. Probl. Miner. Process.*, 53(2017), No. 2, p. 1200.

[6] C.R. Edwards, W.B. Kipkie, and G.E. Agar, The effect of slime coatings of the serpentine minerals, chrysotile and lizardite, on pentlandite flotation, *Int. J. Miner. Process.*, 7(1980), No. 1, p. 33.

[7] B. Feng, J.X. Peng, W.P. Zhang, G.D. Luo, and H.H. Wang, Removal behavior of slime from pentlandite surfaces and its effect on flotation, *Miner. Eng.*, 125(2018), p. 150.

[8] E.R. Bobicki, Q.X. Liu, and Z.H. Xu, Effect of microwave pretreatment on ultramafic nickel ore slurry rheology, *Miner. Eng.*, 61(2014), p. 97.

[9] J. Cao, X.D. Tian, Y.C. Luo, X.Q. Hu, and P.F. Xu, The effect of graphene oxide on the slime coatings of serpentine in the flotation of pentlandite, *Colloids Surf. A*, 522(2017), p. 621.

[10] Y.P. Lu, T. Long, Q.M. Feng, L.M. Ou, and G.F. Zhang, Flotation and its mechanism of fine serpentine, *Chin. J. Nonferrous Met.*, 19(2009), No. 8, p. 1493.

[11] C. Li, C.Y. Sun, Y.L. Wang, Y.F. Fu, P.Y. Xu, and W.Z. Yin, Research on new beneficiation process of low-grade magnesite using vertical roller mill, *Int. J. Miner. Metall. Mater.*, 27(2020), No. 4, p. 432.

[12] P. Tartaj, A. Cerpa, M.T. García-González, and C.J. Serna, Surface instability of serpentine in aqueous suspensions, *J. Colloid Interface Sci.*, 231(2000), No. 1, p. 176.

[13] M. Irannajad, O. Salmani Nuri, and A. Mehdilo, Surface dissolution-assisted mineral flotation: A review, *J. Environ. Chem. Eng.*, 7(2019), No. 3, art. No. 103050.

[14] Y.G. Zhu, G.F. Zhang, Q.M. Feng, D.C. Yan, and W.Q. Wang,

Effect of surface dissolution on flotation separation of fine ilmenite from titanaugite, *Trans. Nonferrous Met. Soc. China*, 21(2011), No. 5, p. 1149.
[15] X.K. Tang and Y.F. Chen, Using oxalic acid to eliminate the slime coatings of serpentine in pyrite flotation, *Miner. Eng.*, 149(2020), art. No. 106228.
[16] M. Alvarez-Silva, *Surface Chemistry Study on Pentlandite–Serpentine System* [Dissertation], McGill University, Montreal, 2010.
[17] Z. Cao, Y.H. Zhang, C.Y. Sun, and Y.D. Cao, Activation mechanism of serpentine by Cu(Ⅱ) and Ni(Ⅱ) ions in copper-nickel sulfide ore flotation, *Chin. J. Nonferrous Met.*, 24(2014), No. 2, p. 506.
[18] P. Patra, T. Bhambani, D.R. Nagaraj, and P. Somasundaran, Dissolution of serpentine fibers under acidic flotation conditions reduces inter-fiber friction and alleviates impact of pulp rheological behavior on Ni ore beneficiation, *Colloids Surf. A*, 459(2014), p. 11.
[19] B.M. Tutolo, A.J. Luhmann, N.J. Tosca, and W.E. Seyfried, Serpentinization as a reactive transport process: The brucite silicification reaction, *Earth Planet. Sci. Lett.*, 484(2018), p. 385.
[20] C. Boschi, A. Dini, I. Baneschi, F. Bedini, N. Perchiazzi, and A. Cavallo, Brucite-driven CO_2 uptake in serpentinized dunites (Ligurian Ophiolites, Montecastelli, Tuscany), *Lithos*, 288-289(2017), p. 264.
[21] H. Ding, S.N. He, J. Cui, and H. Lin, Flotation separation of brucite and serpentine using FL as collector, *Multipurpose Util. Miner. Resour.*, 2(1993), p. 5.
[22] D. Li, J. Jing, and X. Liang, Study on comprehensive utilization of hydrazine serpentine in Ji'an County, Jilin Province, *Build. Mater. Geol.*, 2(1987), p. 30.
[23] D.S. Zhu, *Research on the Flotation for Desilication of High-Silicon Brucite Ore in Kuandian of Liaoning* [Dissertation], Northeastern University, Shenyang, 2011.
[24] Y.F. Fu, Z.L. Zhu, J. Yao, H.L. Han, W.Z. Yin, and B. Yang, Improved depression of talc in chalcopyrite flotation using a novel depressant combination of calcium ions and sodium lignosulfonate, *Colloids Surf. A*, 558(2018), p. 88.
[25] Y.S. Gao, Z.Y. Gao, W. Sun, Z.G. Yin, J.J. Wang, and Y.H. Hu, Adsorption of a novel reagent scheme on scheelite and calcite causing an effective flotation separation, *J. Colloid Interface Sci.*, 512(2018), p. 39.
[26] B. Yang, Z.L. Zhu, H.R. Sun, W.Z. Yin, J. Hong, S.H. Cao, Y. Tang, C. Zhao, and J. Yao, Improving flotation separation of apatite from dolomite using PAMS as a novel eco-friendly depressant, *Miner. Eng.*, 156(2020), art. No. 106492.
[27] Y.F. Fu, W.Z. Yin, B. Yang, C. Li, Z.L. Zhu, and D. Li, Effect of sodium alginate on reverse flotation of hematite and its mechanism, *Int. J. Miner. Metall. Mater.*, 25(2018), No. 10, p. 1113.
[28] W. Jiang, Z.Y. Gao, S.A. Khoso, D.G. Jia, W. Sun, W. Pu, and Y.H. Hu, Selective adsorption of benzhydroxamic acid on fluorite rendering selective separation of fluorite/calcite, *Appl. Surf. Sci.*, 435(2018), p. 752.
[29] J. Schott, O.S. Pokrovsky, and E.H. Oelkers, The link between mineral dissolution/precipitation kinetics and solution chemistry, [in] E.H. Oelkers and J. Schott, eds., *Thermodynamics and Kinetics of Water-Rock Interaction*, Berlin, Boston, 2009, p. 207.
[30] W.Y. Liu, C.J. Moran, and S. Vink, A review of the effect of water quality on flotation, *Miner. Eng.*, 53(2013), p. 91.
[31] F. Rao, I. Lázaro, and L.A. Ibarra, Solution chemistry of sulphide mineral flotation in recycled water and sea water: A review, *Miner. Process. Extr. Metall.*, 126(2017), No. 3, p. 139.
[32] A.C.A. Araújo and R.M.F. Lima, Influence of cations Ca^{2+}, Mg^{2+} and Zn^{2+} on the flotation and surface charge of smithsonite and dolomite with sodium oleate and sodium silicate, *Int. J. Miner. Process.*, 167(2017), p. 35.
[33] W.Z. Yin and Y. Tang, Interactive effect of minerals on complex ore flotation: A brief review, *Int. J. Miner. Metall. Mater.*, 27(2020), No. 5, p. 571.
[34] Q.J. Guan, Y.H. Hu, H.H. Tang, W. Sun, and Z.Y. Gao, Preparation of α-$CaSO_4 \cdot ½H_2O$ with tunable morphology from flue gas desulphurization gypsum using malic acid as modifier: A theoretical and experimental study, *J. Colloid Interface Sci.*, 530(2018), p. 292.
[35] S. Farrokhpay, The importance of rheology in mineral flotation: A review, *Miner. Eng.*, 36-38(2012), p. 272.
[36] C. Li, K. Runge, F.N. Shi, and S. Farrokhpay, Effect of flotation froth properties on froth rheology, *Powder Technol.*, 294(2016), p. 55.
[37] Z.L. Zhu, D.H. Wang, B. Yang, W.Z. Yin, M.S. Ardakani, J. Yao, and J.W. Drelich, Effect of nano-sized roughness on the flotation of magnesite particles and particle-bubble interactions, *Miner. Eng.*, 151(2020), art. No. 106340.
[38] L. Wang, Y. Peng, K. Runge, and D. Bradshaw, A review of entrainment: Mechanisms, contributing factors and modelling in flotation, *Miner. Eng.*, 70(2015), p. 77.
[39] J.J. Wang, W.H. Li, Z.H. Zhou, Z.Y. Gao, Y.H. Hu, and W. Sun, 1-Hydroxyethylidene-1,1-diphosphonic acid used as pH-dependent switch to depress and activate fluorite flotation I: Depressing behavior and mechanism, *Chem. Eng. Sci.*, 214(2020), art. No. 115369.
[40] H.L. Li, W.N. Xu, F.F. Jia, J.B. Li, S.X. Song, and Y. Nahmad, Correlation between surface charge and hydration on mineral surfaces in aqueous solutions: A critical review, *Int. J. Miner. Metall. Mater.*, 27(2020), No. 7, p. 857.
[41] S.Y. Yang, B.H. Xie, Y.P. Lu, and C. Li, Role of magnesium-bearing silicates in the flotation of pyrite in the presence of serpentine slimes, *Powder Technol.*, 332(2018), p. 1.
[42] O. Guven, M.S. Celik, and J.W. Drelich, Flotation of methylated roughened glass particles and analysis of particle-bubble energy barrier, *Miner. Eng.*, 79(2015), p. 125.
[43] J.W. Lu, Z.T. Yuan, J.T. Liu, L.X. Li, and S. Zhu, Effects of magnetite on magnetic coating behavior in pentlandite and serpentine system, *Miner. Eng.*, 72(2015), p. 115.
[44] D. Li, W.Z. Yin, Q. Liu, S.H. Cao, Q.Y. Sun, C. Zhao, and J. Yao, Interactions between fine and coarse hematite particles in aqueous suspension and their implications for flotation, *Miner. Eng.*, 114(2017), p. 74.
[45] J. Ansarinasab and M. Jamialahmadi, Investigating the effect of interfacial tension and contact angle on capillary pressure curve, using free energy Lattice Boltzmann Method, *J. Nat. Gas Sci. Eng.*, 35(2016), p. 1146.
[46] M. Farahat, T. Hirajima, K. Sasaki, and K. Doi, Adhesion of *Escherichia coli* onto quartz, hematite and corundum: Extended DLVO theory and flotation behavior, *Colloids Surf. B*, 74(2009), No. 1, p. 140.
[47] Y.C. Xia, G.Q. Rong, Y.W. Xing, and X.H. Gui, Synergistic adsorption of polar and nonpolar reagents on oxygen-containing graphite surfaces: Implications for low-rank coal flotation, *J. Colloid Interface Sci.*, 557(2019), p. 276.
[48] M. Alvarez-Silva, M. Mirnezami, A. Uribe-Salas, and J.A. Finch, Point of zero charge, isoelectric point and aggregation of phyllosilicate minerals, *Can. Metall. Q.*, 49(2010), No. 4, p. 405.